Received: 31 May 2023 | Revised: 19 December 2023 | Accepted: 20 January 2024

DOI: 10.1002/nbm.5120

RESEARCH ARTICLE

NMR IN BIOMEDICINE WILEY

Reproducibility of absolute quantification of adenosine triphosphate and inorganic phosphate in the liver with localized ^{31}P-magnetic resonance spectroscopy at 3-T using different coils

Marc Jonuscheit[1,2] | Stefan Wierichs[1,2] | Maik Rothe[1,2,3] | Benedict Korzekwa[1,2] | Julian Mevenkamp[4] | Pavel Bobrov[2,5] | Yuliya Kupriyanova[1,2] | Michael Roden[1,2,6] | Vera B. Schrauwen-Hinderling[1,2,4]

[1]Institute for Clinical Diabetology, German Diabetes Center, Leibniz Institute for Diabetes Research at Heinrich Heine University Düsseldorf, Düsseldorf, Germany

[2]German Center for Diabetes Research (DZD e.V.), München-Neuherberg, Germany

[3]University Clinic and Outpatient Clinic for Radiology, University Hospital Halle (Saale), Halle (Saale), Germany

[4]Department of Radiology and Nuclear Medicine, Maastricht University Medical Center, Maastricht, The Netherlands

[5]Institute for Biometrics and Epidemiology, German Diabetes Center, Leibniz Institute for Diabetes Research at Heinrich Heine University Düsseldorf, Düsseldorf, Germany

[6]Department of Endocrinology and Diabetology, Medical Faculty and University Hospital Düsseldorf, Heinrich Heine University Düsseldorf, Düsseldorf, Germany

Correspondence
Vera B. Schrauwen-Hinderling, Metabolic Imaging Group, German Diabetes Center, Auf'm Hennekamp 65, 40225 Düsseldorf, Germany.
Email: vera.schrauwen-hinderling@ddz.de

Abstract

Concentrations of the key metabolites of hepatic energy metabolism, adenosine triphosphate (ATP) and inorganic phosphate (P_i), can be altered in metabolic disorders such as diabetes mellitus. ^{31}Phosphorus (^{31}P)-magnetic resonance spectroscopy (MRS) is used to noninvasively measure hepatic metabolites, but measuring their absolute molar concentrations remains challenging. This study employed a ^{31}P-MRS method based on the phantom replacement technique for quantifying hepatic ^{31}P-metabolites on a 3-T clinical scanner. Two surface coils with different size and geometry were used to check for consistency in terms of repeatability and reproducibility and absolute concentrations of metabolites. Day-to-day ($n = 8$) and intra-day ($n = 6$) reproducibility was tested in healthy volunteers. In the day-to-day study, mean absolute concentrations of γ-ATP and P_i were 2.32 ± 0.24 and 1.73 ± 0.26 mM (coefficient of variation [CV]: 7.3% and 8.8%) for the single loop, and 2.32 ± 0.42 and 1.73 ± 0.27 mM (CVs 6.7% and 10.6%) for the quadrature coil, respectively. The intra-day study reproducibility using the quadrature coil yielded CVs of 4.7% and 6.8% for γ-ATP and P_i without repositioning, and 6.3% and 7.1% with full repositioning of the volunteer. The results of the day-to-day data did not differ between coils and visits. Both coils robustly yielded similar results for absolute concentrations of hepatic ^{31}P-metabolites. The current method, applied with two different surface coils, can be

Abbreviations: ^{31}P, phosphorus; AMARES, advanced method for accurate, robust, and efficient spectral fitting; ATP, adenosine triphosphate; BMI, body mass index; BW, spectral bandwidth; CI, confidence interval; CSD, chemical shift displacement; CV, coefficient of variation; CW, continuous wave; FOV, field of view; Gd-DTPA, gadolinium-diethylenetriaminepentaacetic acid; GDS, German Diabetes Study; GLMM, generalized linear mixed model; GPC, glycero-phosphocholine; GPE, glycero-phosphoethanolamine; HS, hyperbolic secant; ISIS, image-selected in vivo spectroscopy; jMRUI, Java magnetic resonance user interface; K_2HPO_4, dipotassium phosphate; KH_2PO_4, monopotassium phosphate; MeP, methylphosphonic acid; MRS, magnetic resonance spectroscopy; N, sample points; NAD(P)H, nicotinamide adenine dinucleotide (phosphate); NOE, nuclear Overhauser enhancement; NSA, number of signal averages; PC, phosphocholine; PCr, phosphocreatine; PDE, phosphodiester; PE, phosphoethanolamine; PEP, phosphoenolpyruvate; P_i, inorganic phosphate; PME, phosphomonoester; PtdC, phosphatidylcholine; SD, standard deviation; SNR, signal-to-noise ratio; T1DM, type 1 diabetes mellitus; T2DM, type 2 diabetes mellitus; TE, echo time; TR, repetition time; UDPG, uridine diphosphate glucose; VOI, volume of interest.

Funding information
This study was supported in part by the German Diabetes Center (DDZ), which is funded by the Ministry of Culture and Science of the State of North Rhine Westphalia and the German Federal Ministry of Health (BMG), by grants of the Federal Ministry for Research (BMBF) to the German Center for Diabetes Research (DZD e. V.). MR is also supported by grants from the European Community (HORIZON-HLTH-2022-STAYHLTH-02-01: Panel A) to the INTERCEPT-T2D consortium, the German Research Foundation (DFG, GRK 2576) and the Schmutzler-Stiftung. VSH was supported by an ERC starting grant (grant no. 759161 "MRS in diabetes"). The funding sources had no role in study design, data collection, data analysis, data interpretation, or writing of the report.

readily utilized in long-term and interventional studies. In comparison with the single loop coil, the quadrature coil also allows measurements at a greater distance between the coil and liver, which is relevant for studying people with obesity.

KEYWORDS
absolute quantification, hepatic adenosine triphosphate, hepatic inorganic phosphate, reproducibility of ^{31}P-MRS, surface coil

1 | INTRODUCTION

The application of ^{31}phosphorus (^{31}P)-magnetic resonance spectroscopy (MRS) methods for measurements in the liver at clinical field strengths offers novel insights into energy metabolism. ^{31}P-MRS enables the detection of key metabolites such as adenosine triphosphate (γ-, α-, and β-ATP) and inorganic phosphate (P_i), as well as grouped phosphomonoesters (PMEs) and grouped phosphodiesters (PDEs).[1–23] Changes in their hepatic concentrations have been implicated in several diseases such as hepatocellular carcinoma,[1] liver cirrhosis,[1–6] and lymphoma,[7] but also in type 1 diabetes mellitus (T1DM),[8–10] type 2 diabetes mellitus (T2DM),[10–16] and other diseases.[17–19]

Qualitative MRS studies express the intensities of hepatic ^{31}P-metabolites as relative ratios compared with a reference metabolite. Mostly, the ATP signal is used as reference and studies report relative ratios of PME/ATP, PDE/ATP, PME/PDE, and P_i/ATP,[1,2,7,20–22] or ratios of single metabolites relative to the total ^{31}P-metabolite signal.[3,11,23] Assuming a certain concentration for the reference metabolite, for example, a γ-ATP concentration of 2.5–2.65 mmol/L [mM] based on liver biopsy data,[24] ratios can be converted to absolute concentrations.[25–28] The major drawback of this procedure is the variability of the reference metabolite. In that regard, it was previously shown that both hepatic γ-ATP and P_i decrease by approximately 37% in people with alcoholic hepatitis[4] and 25% in people with T2DM,[13] an effect that would have been missed when using ATP as reference. In order to measure tissue concentrations in absolute terms, it is necessary to normalize the obtained signals in a calibration measurement of a phantom with known concentration employing a so-called phantom replacement experiment.[29] Typically, a 2–5 L phantom containing monopotassium phosphate (KH_2PO_4) is measured with the identical protocol and setup as in vivo to take into account several methodological and coil-specific factors, such as coil loading, coil sensitivity, inhomogeneity of the excitation field B_1 and the excitation pulse profile to obtain absolute concentrations.[4,29–32]

The majority of people with T2DM are characterized by overweight or obesity, making the measurement of hepatic ^{31}P-metabolites challenging because of the large distance of the region of interest (liver) from the coil and the limited sensitivity of standard single loop coils. It was reported earlier that obesity is the strongest predictor of failed data acquisition for T2DM and that every unit increase in body mass index (BMI) lowered the amount of successful ^{31}P-MRS by 14%.[11] One possibility to counter this trend is the utilization of coils with improved coil design. For example, quadrature coils consist of multiple coil loops and in theory increase the signal-to-noise ratio (SNR) by a factor of $\sqrt{2}$ and simultaneously halve the necessary transmission power.[33]

For longitudinal cohort studies like the German Diabetes Study (GDS), which investigates the course of diabetes and its subtypes (endotypes) as well as its comorbidities for 20 years,[34,35] liver ATP and P_i are quantified repetitively over a long period of time and thus consistency of values over decades is mandatory. So far, a multipurpose standard single loop coil was used for this purpose in this study. To reduce missing values due to obesity and still guarantee continuity of the measured values, a newly designed quadrature coil was tested and the obtained values were compared with the outcome of the previously used single loop coil. Furthermore, the reproducibility using the new coil was assessed within a single session (intra-day repeatability and reproducibility) and between sessions on different days (day-to-day reproducibility). The latter is important for calculating the sample size in longitudinal studies.

Thus, we aimed (i) to compare the performance and stability of the same ^{31}P-method to detect and quantify hepatic ^{31}P-metabolites in molar concentrations on a 3-T clinical scanner using two different coil designs, a single loop and a quadrature coil; (ii) to evaluate the day-to-day and intra-day reproducibility of this method; and (iii) to assess the potential replacement of the single loop coil by the quadrature coil for its use in clinical intervention and larger cohort studies.

2 | MATERIALS AND METHODS

2.1 | Volunteers

Eleven volunteers (seven males/four females) aged 24 to 56 years, with a broad range of BMI (20.6–32.4 kg/m^2), participated in this study (Table 1). The study was approved by the local ethics committee and all volunteers gave their written informed consent before participation in the study.

2.2 | Study design

Two surface coils with different coil geometry (single loop and quadrature) and from different manufacturers were used to determine absolute values of ^{31}P-metabolites and day-to-day reproducibility. Furthermore, the quadrature coil was used to determine the intra-day repeatability and reproducibility of ^{31}P-metabolites assessment and was compared with the intra-day reproducibility as determined for the single loop coil in an earlier study.[36] The study design is visualized in Figure 1.

2.2.1 | Day-to-day reproducibility

Eight volunteers aged 27 to 56 years, with a BMI range of 20.8–32.4 kg/m^2, underwent ^{31}P-MRS of the liver in three visits each within a week (4 to 7 days, stated as V1–V3 in Figure 1A; Table 1). To achieve standardized physiological conditions, each volunteer was measured at the same time of the day after a 4.5-h fast. Moreover, volunteers were requested to record their food intake before the first examination to replicate their diet prior to the following measurement days. All participants were asked to refrain from strenuous exercise as well as from alcohol and caffeine intake on the day preceding the examination. Volunteers were repositioned every time before switching the coil to enhance their comfort, secure full repositioning, and reset scanner adjustments.

For the quadrature coil, long-term reproducibility was also tested in five out of the eight volunteers. These volunteers participated in a fourth visit (Figure 1A, V4) after approximately 3 months (11 to 14 weeks after the third measurement) to reassess metabolite concentrations (Table 1).

2.2.2 | Intra-day repeatability and reproducibility

To assess the intra-day repeatability and reproducibility of the ^{31}P-MRS measurements acquired with the quadrature coil, a subgroup of six healthy volunteers (Table 1) aged 24 to 50 years, with a BMI range of 20.6–29.4 kg/m^2, was examined several times within a day to judge methodological variations (Figure 1B). The first five spectra were consecutively acquired to assess (a) repeatability without coil repositioning ($n = 6$, Figure 1B, M1–M3); and (b) reproducibility of voxel replacement ($n = 3$, Figure 1B, M3–M5) to account for sensitivity of the method regarding different placement of the volume of interest (VOI) while the volunteer was not moved. Next, two more measurements ($n = 6$, Figure 1B, M6–M7) with full volunteer repositioning and "optimal" VOI placement, just as in M1-M3, were acquired to evaluate reproducibility with coil repositioning. For this, the volunteers were asked to leave the scanner each time for a break of 5 min. Additionally, no markers for coil positioning

TABLE 1 Participants' characteristics. A total of eight volunteers participated in the three-visit day-to-day study. Longitudinal day-to-day and intra-day repeatability and reproducibility were assessed in groups of $n = 5$ and $n = 6$, respectively. All values are reported as mean ± SD.

	^{31}P day-to-day variability liver (3 visits)	^{31}P day-to-day variability liver (4 visits)	^{31}P intra-day variability liver (1 visit)
No. of volunteers	8	5	6
Sex (male/female)	7/1	4/1	2/4
Age (years)	37.1 ± 11.0	29.6 ± 2.1	34.2 ± 9.6
Weight (kg)	91.4 ± 17.4	85.8 ± 20.3	80.0 ± 21.1
Height (m)	1.83 ± 0.11	1.84 ± 0.13	1.77 ± 0.15
BMI (kg/m^2)	27.3 ± 4.2	25.2 ± 3.8	25.3 ± 3.5
Coil used	Single loop and quadrature	Quadrature	Quadrature
Data used for	Day-to-day reproducibility + coil comparison	Day-to-day reproducibility	Intra-day repeatability and reproducibility

Abbreviation: BMI, body mass index.

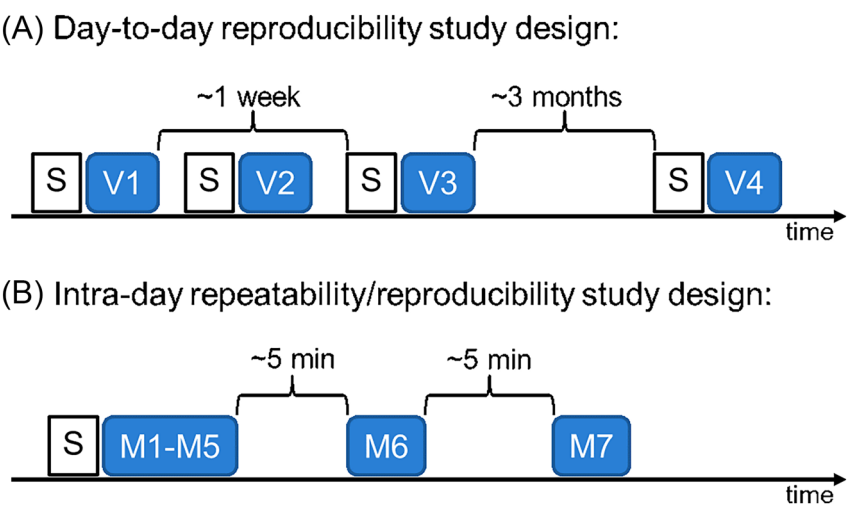

FIGURE 1 Study design. S, standardization protocol including measurement at the same time of the day and 4.5-h fasting after standard meal. (A) Day-to-day reproducibility study: hepatic ^{31}P-metabolites were measured with ^{31}P-MRS at each visit V1–V4 (V1–V3 within 1 week using both single loop and quadrature coils, V4 after 3 months using only the quadrature coil). (B) Intra-day repeatability/reproducibility study (quadrature coil only): M1–M5, five consecutive ^{31}P-measurements to evaluate (i) repeatability of the method without coil repositioning (M1–M3); and (ii) sensitivity of the method regarding different volume of interest (VOI) placement (M3–M5). M6 and M7 denote additional measurements to evaluate reproducibility of the method with coil repositioning; just as for M1–M3, the most optimal VOI position was sought.

were used, to guarantee a full repositioning with new adjustments. Moreover, the same physiological standardization protocol as in the day-to-day sessions was applied. Intra-day reproducibility of the single loop coil was previously reported by our group.[36]

2.3 | MR system and surface coils

All the examinations were conducted on a clinical 3-T MR system with the multinuclear option (bore diameter 60 cm, Philips Achieva dStream, Best, the Netherlands) using two different surface coils (Figure 2C,F). The first coil was a vendor-provided flat 14-cm circular single loop ^{31}P-surface coil (transmit-receive coil; Philips Healthcare, Best, the Netherlands) and the second coil was a newly designed curved quadrature ^{31}P-surface coil (transmit-receive coil; RAPID Biomedical, Rimpar, Germany) with total ^{31}P-loop size of 220 mm × 160 mm. Shimming, ^{1}H decoupling, and nuclear Overhauser enhancement (NOE) were performed by the ^{1}H-body coil (transmit-receive birdcage coil; Philips Healthcare). To correct for coil loading effects, both ^{31}P-coils had notches where methylphosphonic acid (MeP)-filled glass spheres were positioned inside the housing. While the MeP reference of the single loop coil was provided by the manufacturer and located in a sealed cavity in the center of the 140 mm loop, the MeP (98%, Sigma-Aldrich, Schnelldorf, Germany) references of the quadrature coil were custom made using two 530 µL spheres, whereas one is placed in the center of each ^{31}P-loop (the positions are highlighted in red in Figure 2C,F).

2.4 | Acquisition and localization of the ^{31}P-signal in human liver

First, scout images in three orientations were acquired (five slices of 15 mm thickness, 10 mm gap, field of view [FOV] 450 × 450 mm^2) followed by transverse T_2-weighted images acquired with multislice 2D single-shot turbo spin echo (repetition time [TR]/echo time [TE] 883/80 ms; 23 slices of 6mm thickness, 1mm gap, FOV 450 × 378 mm^2). After verification of correct coil positioning on the right lateral lobe of the liver, ^{31}P-MRS acquisition was planned by carefully placing a 60 × 60 × 60 mm^3 VOI within the liver tissue, avoiding immediate proximity to the lung, gallbladder, and abdominal muscle. Liver spectra were acquired using a 3D-localized image-selected in vivo spectroscopy (ISIS)[37] sequence with a 5.43 or 3.83 ms hyperbolic secant (HS) adiabatic half passage pulse for excitation (excitation bandwidth 1.15 or 1.63 kHz) for the single loop and quadrature coil, respectively, TR 6 s, number of signal averages (NSA) 128, total acquisition time 13 min, sample points (N) 2048, spectral bandwidth (BW) 3 kHz, excitation pulse center ∼1.0 ppm, broadband decoupling (WALTZ-4) with offset frequency −100 Hz and B_1 amplitude 7 µT, continuous wave (CW) NOE with mixing time 3500 ms, offset frequency −100 Hz, and B_1 amplitude 0.5 µT. The duration of the HS inversion pulse for slice selection was 5.66 and 4.0 ms, while the HS inversion bandwidth was 2.25 and 3.18 kHz for the single loop and quadrature coil, respectively. No respiratory triggering was used. Shimming typically reached a linewidth of ∼30 Hz for both coils.

Spectra of the external reference MeP spheres were acquired to account for coil loading in separate scans using a pulse-acquire sequence with the identical HS adiabatic pulse of the corresponding coil for excitation, TR 8 s, NSA 16, total acquisition time ∼2 min, N 8192, BW 6 kHz,

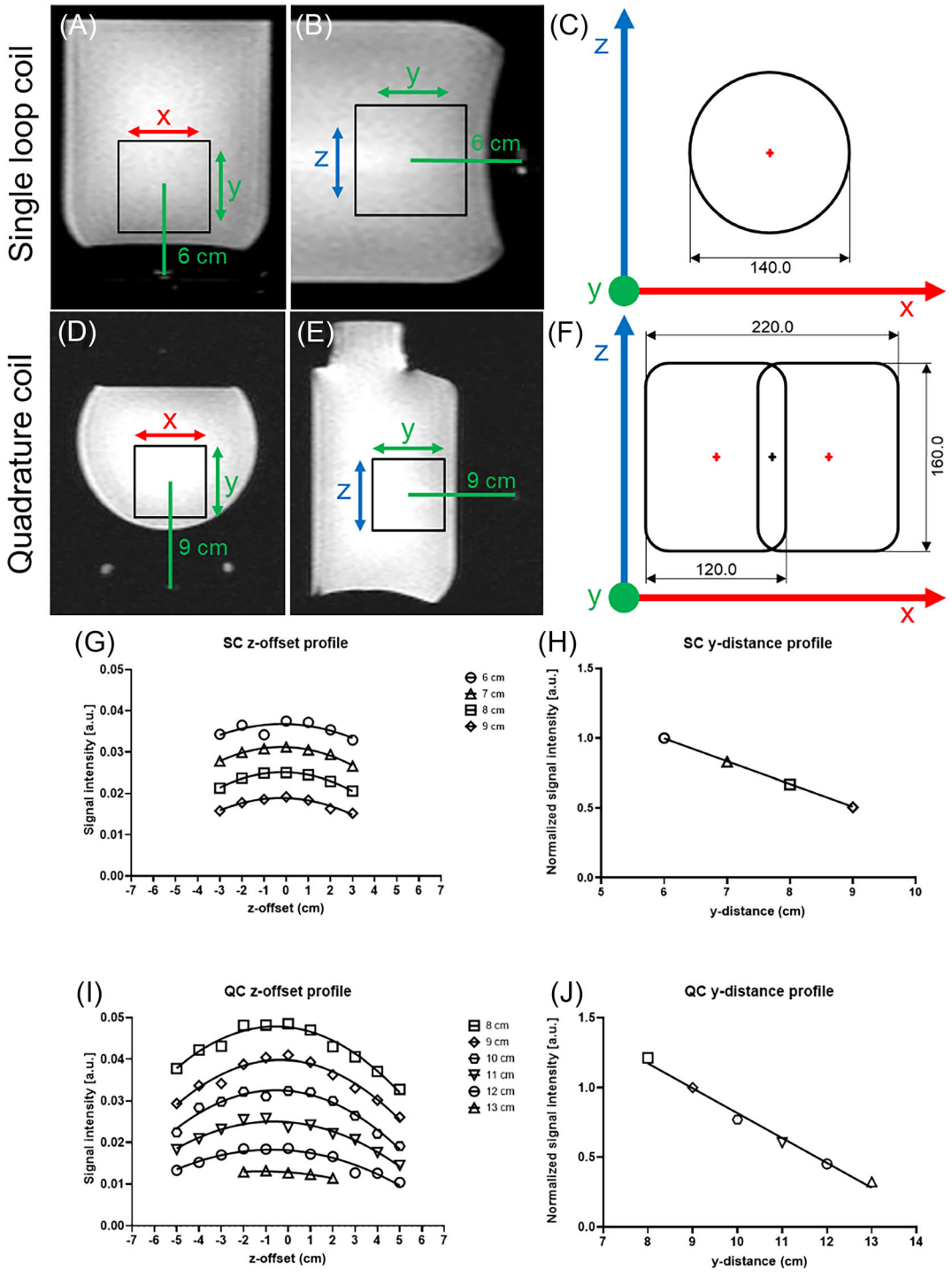

FIGURE 2 In vitro setup to determine correction factors for absolute quantification. The volume of interest (VOI) was shifted in all dimensions to compensate for different placements in the liver. For the single loop coil setup the phantom was placed upright on the coil (A, B), while it was laid down for the quadrature coil setup due to its curved housing (D, E). (C, F) Schematic overview of both ^{31}P-coil designs including coil orientation for (C) flat circular single loop, and (F) curved quadrature coil. Reference cavities are visualized as crosses. Red crosses highlight the location of the MeP spheres in the coil, the black cross symbolizes a sphere filled with water. All displayed dimensions are expressed in mm. (G, I) Offset profile of both coils to account for imperfect placement of the VOI in the central position of the coil. (H, J) Depth profile of both coils to account for variations in distance between VOI and the central coil reference. MeP, methylphosphonic acid; SC, single loop coil; QC, quadrature coil.

no proton decoupling, NOE, or localization. Shim voxel size was adjusted to the position of the external reference and varied in size for the two coils (single loop 80 × 80 × 80 mm^3, quadrature coil 130 × 80 × 80 mm^3). All details of the acquisition procedure are listed in Table S1.[38]

2.5 | ^{31}P-MRS in vitro measurements and correction factors for absolute quantification

In order to enable absolute quantification of ^{31}P-metabolites in the liver, an in-house mixed phantom containing 50 mM dipotassium phosphate (K_2HPO_4) (Sigma Aldrich) and 0.1 mM gadolinium-diethylenetriaminepentaacetic acid (Gd-DTPA) (Sigma Aldrich) was measured as matching phantom (cylindrical phantom, volume 3 L, diameter 16 cm, height 19 cm, T_1 10.36 s).[36] The phantom was placed in a similar position inside the scanner as the liver and spectra were acquired with the same geometries and parameters as used for the in vivo protocol (Figure 2A,B,D,E).

Spectra were acquired while the distance between the VOI and central coil reference (y-distance) varied, ranging from 6 to 10 cm in 1 cm steps (Figure 2H). In each of these steps, nine different frequency offsets corresponding to the position of the prominent ^{31}P-metabolites were set to be able to correct for the pulse profile (Figure S1). Additionally, to account for imperfect placement in the central position of the coil of the VOI, further spectra with positions towards the edge of the coil, ranging from −3 to 3 cm in 1 cm steps, were acquired (Figure 2G). In the final quantification table, these profiles allow to correct the in vivo spectrum resonances regarding offset frequency for each individual peak and x-, y-, and z-distance for each volunteer and metabolite.

Because of the different size and geometry of the quadrature coil, spectra for distance correction ranged from 8 to 13 cm (1 cm steps) and VOI placement towards the edge of the coil from −5 to 5 cm in steps of 1 cm, respectively (Figure 2I,J).

2.6 | Quantification procedure using the phantom replacement method

Absolute quantification of ^{31}P-metabolites in molar concentration was achieved using the phantom replacement method as introduced by Meyerhoff et al.[29] For correction of coil loading, the signal from the small glass sphere(s) containing MeP located in the coil housing was used.

In summary, corrections were applied for coil loading, T_1 relaxation times, the excitation profile of the adiabatic pulse, and B_1 inhomogeneities of the surface coil in all three spatial directions. The final concentration c^{ij} (in mM) of each corresponding ^{31}P-metabolite i of volunteer j can be obtained by the following equation[36]:

$$c^{ij} = \frac{A^{ij}}{A_{ph}} \cdot \frac{A^{ph}_{ref}}{A^{j}_{ref}} \cdot c_{ph} \cdot f^{i}_{T_1} \cdot f^{i}_{offset} \cdot f_{B_{1,xyz}} \cdot f_{liver\ lipid\ content}$$

A^{ij} represents the fitted peak area of a ^{31}P-metabolite in the liver of a volunteer, A_{ph} is the fitted peak area of the K_2HPO_4 phantom, which is corrected for T_1 and temperature, A^{ph}_{ref} denotes the fitted peak area of the MeP reference in the phantom measurement, A^{j}_{ref} is the fitted peak area of the MeP reference in a volunteer measurement, c_{ph} represents the known concentration of K_2HPO_4 in mM (50 mM), f^{i}_{T1} is referred to the correction factor for the corresponding T_1 relaxation time of the ^{31}P-compound, f^{i}_{offset} is the correction factor accounting for signal intensity of the different chemical shifts of the metabolites due to the nonuniform excitation pulse profile, $f_{B1,xyz}$ denotes the correction factor for the distance between the center of the coil to the center of the voxel in all three spatial directions, and $f_{liver\ lipid\ content}$ represents the correction factor for the amount of liver lipid content.

T_1 relaxation times of the ^{31}P-metabolites in the liver were corrected by using the reported values at 3-T by Schmid et al.[27] A correction for hepatic lipid content was not applied in this study. As volunteers were scanned within a short time period when they did not change their nutritional behavior, we assumed that the hepatic lipid content was the same in each session and did not influence reproducibility.

2.7 | Data processing

In line with best practice,[38,39] all spectra were reviewed regarding quality and were processed in a blinded fashion to the origin of the spectra (volunteer and session no.). To ensure good data quality, all spectra were analyzed regarding SNR using the definition[39] $SNR = \frac{Signal}{\sigma_{Noise}}$. After application of a 15 Hz Gaussian filter, the signal was defined as the fitted amplitude of the metabolite of interest and noise (σ) as standard deviation (SD) of the spectrum between 10 and 20 ppm both in the frequency domain using a custom written MATLAB script (MathWorks Inc. R2021a, Natick, MA, USA). Two quality criteria were applied: SNR of γ-ATP less than 4 and SNR of P_i less than 2.5 as marker for low spectral quality. Moreover, to account for potential signal contamination from abdominal skeletal muscle, the phosphocreatine (PCr) to γ-ATP peak ratio was calculated and spectra with PCr/γ-ATP more than 0.5 were excluded.

Spectra were processed using Java magnetic resonance user interface (jMRUI) software.[40,41] All spectra were apodized with a Gaussian line shape of 15 Hz, manually zero order-phased and frequency adjusted by setting the γ-ATP resonance to −2.48 ppm. Peak fitting was performed using

the advanced method for accurate, robust, and efficient spectral fitting (AMARES)[42,43] algorithm in jMRUI. Twelve peaks were quantified to account for 11 hepatic metabolite resonances and one additional peak to additionally account for potential PCr contamination from abdominal muscles. Chemical shift assignment was adapted from previous publications[44,45] and a custom-created prior knowledge file was used for fitting (Table S2).

The external reference spectra were processed using a 20 Hz Gaussian line shape apodization and manual zero order phasing. Next, the resonance of MeP was fitted as a single Gaussian peak, whereas amplitude, linewidth, and frequency were not constrained (set to "estimated").

2.8 | Statistical analysis

Statistical analysis was performed with GraphPad Prism v. 9.5 for Windows (GraphPad Software, San Diego, CA, USA). All reported data for absolute concentrations of ^{31}P-metabolites are presented as mean ± SD or mean (95% confidence interval [CI]). To assess the intra-volunteer variability, the coefficient of variation (CV), defined as the ratio of the SD to the mean, was calculated for all ^{31}P-measurements. Bland–Altman analysis was performed to assess the agreement between concentrations obtained for γ-ATP and P_i using both coils.

In order to test for significant differences in the estimated absolute quantification results obtained from the two different coils in the day-to-day reproducibility study (three visits with both coils), an analysis of covariance (ANCOVA) for generalized linear mixed model[46] (GLMM) with repeated measures adjusted for both coil and visit was performed in SAS v. 9.4 for Windows (SAS Institute, Cary, NC, USA) with significance level $\alpha = 0.05$.

3 | RESULTS

3.1 | ATP and P_i concentration

Valid results were obtained for ATP and P_i from all participants, on all occasions, except for one spectrum acquired during day-to-day measurements with the single loop coil, which was excluded due to low SNR. The mean absolute concentrations of γ-ATP and P_i were similar for both coils, amounting to 2.32 ± 0.24 and 1.73 ± 0.26 mM for the single loop and 2.32 ± 0.42 and 1.73 ± 0.27 mM for the quadrature coil, respectively (n.s., Tables 2 and 3). Values are given as the mean ± SD of the three measurement days. The Bland–Altman comparison of inter-coil variability shows a mean difference in concentration between both coils of −0.00522 ± 0.398 mM for γ-ATP and 0.000870 ± 0.233 mM for P_i (Figure 3). Of the 23 compared pairs of values, 22 (95%) and 21 (91%) were within 2 SDs for γ-ATP of P_i, respectively. Taking into account data from the fourth measurement, acquired approximately 3 months later, did not significantly change the results for γ-ATP (2.42 ± 0.45 mM) and P_i (1.76 ± 0.31 mM). Even although the main focus of this study was on assessing γ-ATP and P_i, for completeness we also analyzed the other prominent ^{31}P-metabolites glycero-phosphocholine (GPC), glycero-phosphoethanolamine (GPE), phosphocholine (PC), and phosphoethanolamine (PE) regarding metabolite concentrations, CVs, and statistical differences between both coils (Tables S3–S5).

3.2 | Variability of ATP and P_i

The mean intra-volunteer CVs of the three sessions day-to-day reproducibility study of γ-ATP and P_i were 7.3% ± 3.1% and 8.8% ± 3.4% for the single loop and 6.7% ± 3.3% and 10.6% ± 11.3% for the quadrature coil, respectively. Taking into account the fourth measurement after 3 months, the

TABLE 2 Estimated CVs and absolute concentrations of γ-ATP and P_i of the day-to-day and intra-day repeatability and reproducibility studies of the ^{31}P-MRS method including both coils.

	No. of volunteers	% CV intra-volunteer ± SD		Concentration, mM (mean ± SD)	
		γ-ATP	P_i	γ-ATP	P_i
Single loop coil—three sessions (V1–V3)	8	7.3 ± 3.1	8.8 ± 3.4	2.32 ± 0.24	1.73 ± 0.26
Quadrature coil—three sessions (V1–V3)	8	6.7 ± 3.3	10.6 ± 11.3	2.32 ± 0.42	1.73 ± 0.27
Quadrature coil—four sessions (V1–V4)	5	6.5 ± 3.7	15.2 ± 8.6	2.42 ± 0.45	1.76 ± 0.31
Quadrature coil—single session without repositioning (M1–M3)	6	4.7 ± 2.2	6.8 ± 2.1	2.24 ± 0.28	1.62 ± 0.25
Quadrature coil—single session with different VOI placement (M3–M5)	3	7.4 ± 2.0	8.2 ± 2.7	2.24 ± 0.22	1.40 ± 0.18
Quadrature coil—single session with volunteer repositioning (M1, M6, M7)	6	6.3 ± 5.3	7.1 ± 6.1	2.35 ± 0.32	1.69 ± 0.27

Abbreviations: CV, coefficient of variation; VOI, volume of interest.

TABLE 3 Analytical results using a repeated measures ANCOVA for GLMM adjusted for both coil and visit for the metabolites γ-ATP and P_i of the single loop and quadrature coil day-to-day reproducibility study (three visits). Estimated absolute concentrations of γ-ATP and P_i with 95% CI are listed for each individual coil or visit and their individual differences are shown.

	Concentration, mM (95% CI)	
Effect	**γ-ATP**	**P_i**
Least squares means		
All spectra of SC coil	2.31 [2.10; 2.53]	1.73 [1.58; 1.87]
All spectra of QC coil	2.32 [2.11; 2.53]	1.73 [1.59; 1.87]
Visit 1 (SC and QC)	2.28 [2.05; 2.50]	1.68 [1.52; 1.83]
Visit 2 (SC and QC)	2.34 [2.12; 2.56]	1.77 [1.61; 1.92]
Visit 3 (SC and QC)	2.34 [2.11; 2.56]	1.75 [1.58; 1.91]
Differences of least squares means		
SC–QC	−0.00554 [−0.146; 0.135]	−0.00066 [−0.131; 0.129]
Visit 1–Visit 2 (SC and QC)	−0.0618 [−0.231; 0.108]	−0.0899 [−0.247; 0.0671]
Visit 1–Visit 3 (SC and QC)	−0.0591 [−0.232; 0.114]	−0.0696 [−0.230; 0.0905]
Visit 2–Visit 3 (SC and QC)	0.00263 [−0.170; 0.175]	0.0203 [−0.140; 0.180]

Abbreviations: ANCOVA, analysis of covariance; CI, confidence interval; GLMM, generalized linear mixed model; QC, quadrature coil; SC, single loop coil.

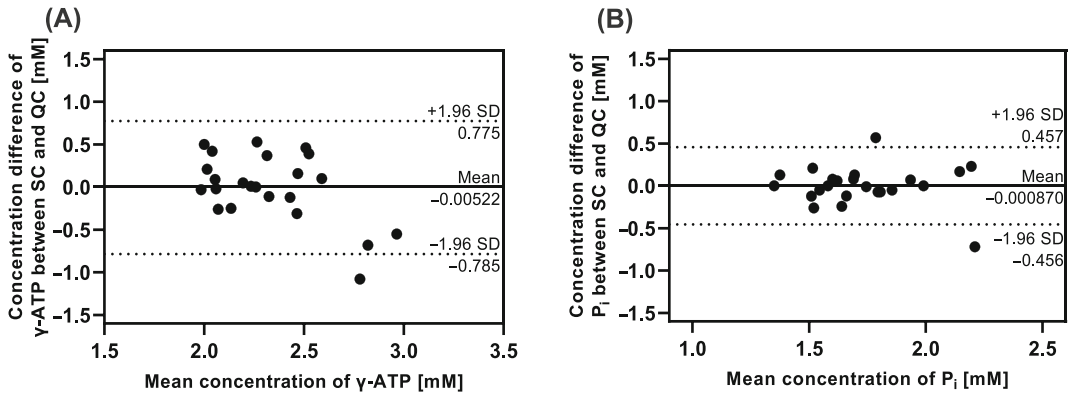

FIGURE 3 Bland–Altman plots for intercoil variability of (A) γ-ATP, and (B) P_i concentrations. 22 out of 23 datapoints are within 2 SDs for γ-ATP and 21 out 23 points for P_i. SC, single loop coil; QC, quadrature coil.

CVs were similar, with 6.5% ± 3.7% for γ-ATP and 15.2% ± 8.6% for P_i. For the intra-day reproducibility, the mean CVs of γ-ATP and P_i amounted to (a) 4.7% ± 2.2% and 6.8% ± 2.1% in a single session without repositioning; (b) 7.4% ± 2.0% and 8.2% ± 2.7% in a single session with different VOI placement; and (c) 6.3% ± 5.3% and 7.1% ± 6.1% in a single session with full repositioning of the volunteer, respectively (Figure 4). An overview of individual obtained values for other prominent ^{31}P-metabolites including the main CVs can be reviewed for both coils in Figure S2.

3.3 | Spectral quality

The mean SNRs of γ-ATP and P_i in the day-to-day study (three visits) were 8.2 ± 1.5 and 7.3 ± 2.3 for the single loop and 8.0 ± 1.5 and 6.8 ± 1.9 for the quadrature coil, respectively. The PCr signal, which indicates signal contamination from muscle, was low in all cases (18% ± 16% and 25% ± 12% of ATP signal intensity for the single loop and quadrature coil, respectively). Figure 5 shows representative ^{31}P-MRS spectra with all 11 prominent hepatic ^{31}P-metabolites.

4 | DISCUSSION

This study used a slightly modified version of an established ^{31}P-MRS method, allowing robust absolute quantification of hepatic γ-ATP and P_i concentrations within 15 min at 3-T with a quadrature coil. Results were compared with the results obtained with the previously used single loop

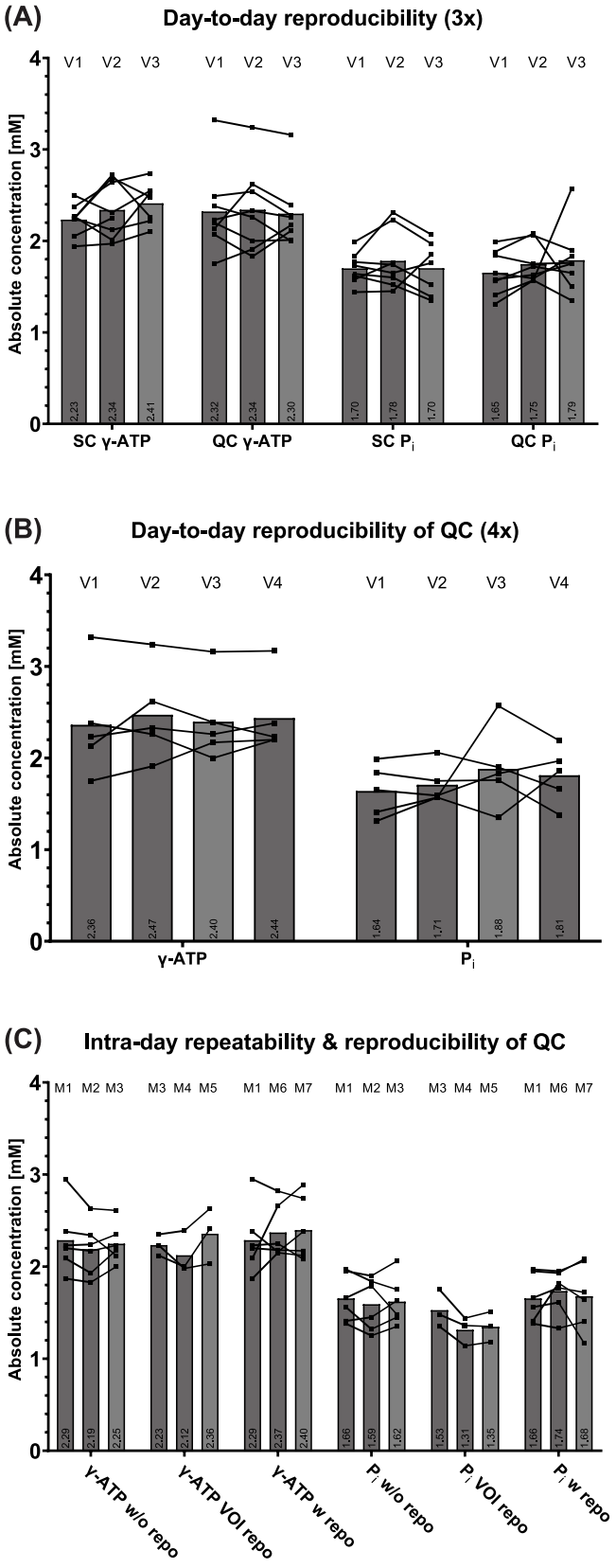

FIGURE 4 Legend on next page.

FIGURE 4 Results of the day-to-day (three and four visits) and intra-day repeatability and reproducibility study. For each study all obtained metabolite concentrations are denoted as a single datapoint. Black bars indicate mean values of one visit or session. Metabolite concentrations are presented in mM concentrations, quantified by the replacement method using a phantom with known concentration. (A) Results of the day-to-day reproducibility study to assess absolute concentrations of γ-ATP and P_i with both coils. All volunteers underwent the same MR sessions on three different days within a week (V1–V3). (B) Results of the day-to-day reproducibility study of the quadrature coil (V1–V3) with an additional measurement approximately 3 months later (V4) to assess the long-term variability of γ-ATP and P_i concentration. (C) Results of the intra-day repeatability and reproducibility study of the quadrature coil. Repeatability and reproducibility of measurements (i) without volunteer repositioning; (ii) with volume of interest (VOI) repositioning; and (iii) with volunteer repositioning between measurements were assessed. SC, single loop coil; QC, quadrature coil.

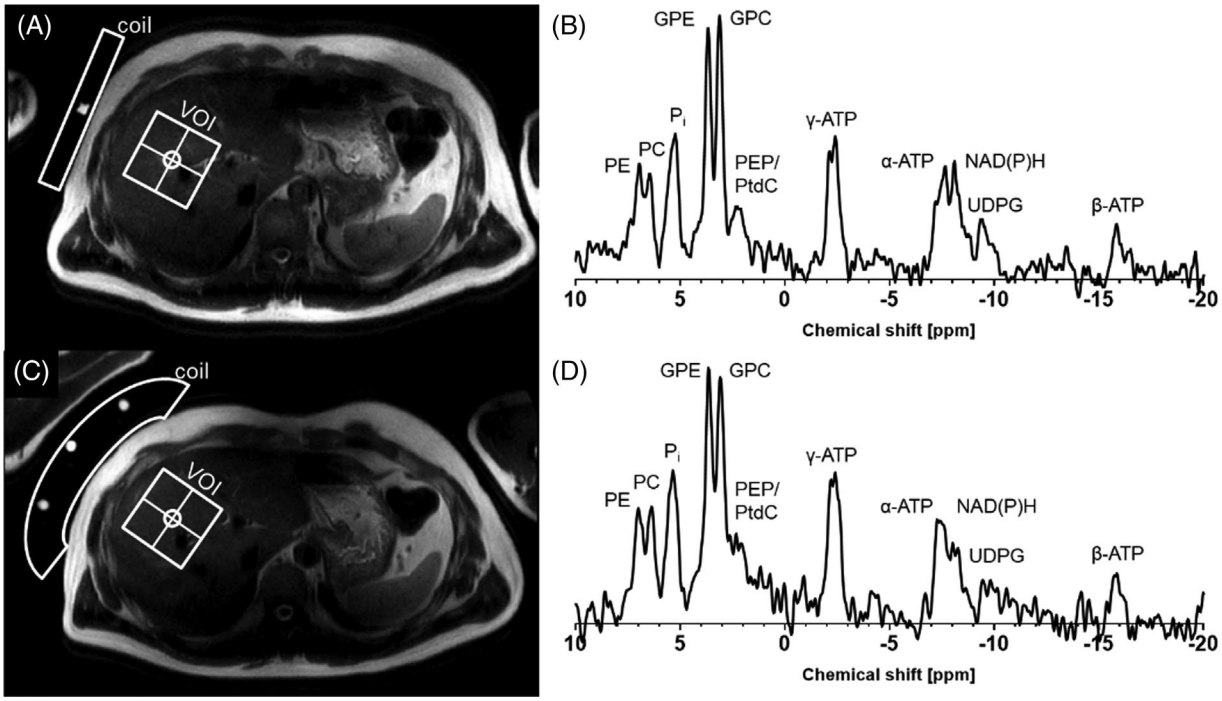

FIGURE 5 Top: single loop coil, bottom: quadrature coil. (A, C) Transversal slices of the liver showing coil placement and position of the volume of interest (VOI). White dots within the coil housing show the position of the reference spheres. (B, D) Representative ^{31}P-MR spectra (apodization 15 Hz) of human liver at a field of 3-T. ATP, α-,β-,γ-adenosine triphosphate; GPC, glycero-phosphocholine; GPE, glycero-phosphoethanolamine; NAD(P)H, nicotinamide adenine dinucleotide (phosphate); P_i, inorganic phosphate; PC, phosphocholine; PE, phosphoethanolamine; PEP/PtdC, phosphoenolpyruvate/phosphatidylcholine; UDPG, uridine diphosphate glucose.

surface coil,[36] and excellent agreement was found between the two coils. The consistency of measurements of absolute concentrations of metabolites in prospective studies over years to decades, like the GDS cohort,[34] can be challenging because coil replacement during the study is inevitable. If a new coil is introduced, the consistency of the results always needs careful validation. This is even more so when the coil geometry is changed. By introducing a slightly larger quadrature coil, we aimed to increase the success rate of hepatic ^{31}P-measurements in people with obesity while making sure that the measured ATP and P_i concentrations were not affected. Measurements in people with obesity using the single loop coil often fail, especially for a high distance between coil and VOI, which results in low SNR and therefore poor quality spectra.

Our results show that the absolute concentrations of ATP and P_i were very similar for both the single loop and quadrature coil and therefore the quadrature coil can indeed replace the single loop coil. This shows the importance of the exact procedures in terms of phantom setup and quantification of spectra, as this seems to be a more important source of variation than the coil used. Indeed, the range reported at different field strengths in the literature is rather large, with 1.39–3.7 mM for γ-ATP and 1.18–2.8 mM for P_i[5,6,8,12,13,17,18,29–32,36,44,47–49] suggesting that differences in site-specific procedures introduce relevant biases. However, the values of this study are well in range with those concentrations reported by other groups.[6,13,18,31,32,36,48]

In terms of quality of the measurement, the coils also performed very similarly. The mean intra-volunteer CVs for both coils were very similar (7.3% and 6.7% for γ-ATP and 8.8% and 10.6% for P_i) and agree with the literature,[1,11,32] which is the typical range for in vivo MRS measurements. The larger coil element size in the quadrature coil was expected to introduce more noise; however, the quadrature geometry should compensate for this by increasing the sensitivity and, therefore, also the signal. Indeed, the SNR results show a very similar outcome for both coils with mean SNRs of γ-ATP and P_i of 8.2 and 7.3 using the single loop and 8.0 and 6.8 using the quadrature coil, respectively.

A fourth measurement in five volunteers after approximately 3 months did not introduce additional variation, showing that basal concentrations of γ-ATP and P_i remain stable in healthy volunteers and when using a simple standardization protocol.

One of the volunteers showed a large deviation in P_i and especially in γ-ATP concentrations using the quadrature coil compared with the results obtained with the single loop coil. In the Bland–Altman analysis, the three most negative outliers for γ-ATP and the most negative point in the P_i plot can be assigned to him. This may originate from difficulties with consistent coil positioning in this volunteer. Being very lean and having a small waist circumference, the rigid, curved design of the quadrature coil did not fit to the volunteer's abdomen, and, during fasting, one of the coil elements was always at a greater distance, with a large air gap between the coil and the body. This appears to be a disadvantage of the quadrature coil, which was intentionally designed to perform ^{31}P-MRS in people with overweight or obesity, and reveals limitations for lean people with a small waist circumference due to its geometry.

Methodological variation, for example, due to respiratory motion or differences in shim, was determined by the consecutive repetition of the protocol (without repositioning). Intra-volunteer CVs of 4.7% for γ-ATP and 6.8% for P_i highlight that the method is highly reproducible and comparable with the literature.[32]

Robustness of the method for nonoptimal VOI placement was checked by purposely placing the VOI in a suboptimal position. In such cases, we detected an increase in CVs to 7.4% and 8.2% for γ-ATP and P_i. These are the highest CVs detected in the intra-day measurements. Although this variability is somewhat higher than with a consistent voxel position, it can still be acceptable for physiological studies and demonstrates that the method can compensate for small deviations from the most ideal VOI placement.

The CVs after full repositioning of the volunteer were slightly higher with 6.3% and 7.1% for γ-ATP and P_i than without repositioning (4.7% and 6.8%), but still below CVs of the day-to-day study (6.7% and 10.6%). Laufs et al.[36] reported comparable intra-day CVs of 9% and 7% assessed in five volunteers twice on different days with three scans including full repositioning. These values are of importance for sample size calculations for interventional studies where volunteers enter the scanner on different days.

In the current study, only one out of 86 spectra had to be excluded due to low SNR. The excluded spectrum was acquired with the single loop coil and excluded because of low SNR (γ-ATP < 4). It should be mentioned that no spectrum was excluded due to an inacceptable degree of abdominal muscle signal contamination resulting in a prominent PCr resonance (PCr/γ-ATP > 0.5). To minimize muscle contamination, a gap between abdominal muscle tissue and VOI was always maintained (Figure 5). Similarly, attempts were made to avoid the gallbladder as much as possible, although this was not always possible because of the limited liver size and the voxel size that was used. It was reported earlier that the resonance at ∼2.06 ppm originates mainly from the gallbladder, which is why it can be used for estimation of signal contamination.[50,51] A voxel size of 60 mm in each direction was applied to achieve a reasonable SNR within a scan time of approximately 13 min. Because a significant number of our cohort study in which this protocol is applied are overweight or obese, the big voxel size is necessary to compensate for signal loss due to the high distance between coil and liver tissue, which would otherwise lead to noisy spectra. In terms of chemical shift displacement (CSD), the chemical shift between γ-ATP and P_i amounts to ∼7.7 ppm, corresponding to ∼400 Hz at 3-T and will result in a CSD of ∼6.7 mm between these two metabolites. As the center of the HS AHP excitation pulse is located between the two metabolites, the CSD will be lower in our experiments, but in opposite directions. When planning measurements, care was taken that the voxel position was well within the liver for both metabolites. Although small, it is important to note that the CSD is taken into account for the absolute quantification, as the in vitro measurements are performed with the same settings as the in vivo measurements.

The main objective of this study was the comparison between two different surface coils for assessing hepatic γ-ATP and P_i. However, it is also possible to gain information about other prominent ^{31}P-metabolites from the acquired spectra. This study used γ-ATP as ATP representative for ATP concentration, although it should be noted that the γ-ATP signal contains a contribution of β-ADP.[52] The only pure ATP resonance is the β-ATP signal; however, due to the big chemical shift of the β-ATP resonance and the limited excitation pulse bandwidth, which resulted in low SNR for β-ATP, it was not possible to reliably quantify this peak. The remaining prominent metabolites GPC, GPE, PC, and PE were also analyzed between both coils and no significant differences were found between both individual visits and coils, except for a difference between the first two visits for GPC and between both coils for GPE (Tables S3 and S4). Furthermore, the CVs of GPC and GPE were less than 10% in the day-to-day study, whereas PC and PE showed more variations (CVs < 20%) (Table S5). Here, the trend also shows that the inaccuracy of the determination of concentrations increases with larger chemical shifts from the excitation pulse center.

This study used jMRUI with the AMARES algorithm for data processing and peak fitting. Establishing custom prior knowledge files including chemical shifts, linewidths, and line shapes allowed both a precise and highly reproducible fitting as well as a fast analysis (Figure 6). Consistent analysis is important, because in the early beginning of employing absolute quantification in liver, the results reported diverged significantly,[6,29,30,44] which was found to be partly caused by differences in processing and quantification methods.[25] Including fitting of the minor resonances uridine diphosphate glucose (UDPG), nicotinamide adenine dinucleotide (phosphate) (NAD(P)H), PCr, phosphoenolpyruvate (PEP), and phosphatidylcholine (PtdC) led to an almost flat residue (Figure 6, top section). PCr, fitted as peak 6, was always included in the fitting procedure as an indicator for signal contamination from superficial muscle and was used as the basis for exclusion of spectra. Noticeable is a continuous decrease of peak amplitude of the three ATP resonances from γ- to α- and especially β-ATP, which is caused by the limited excitation bandwidth (1.15 and 1.63 kHz) of the HS adiabatic pulse of the single loop and quadrature coil and the fact that the center frequency was set in between the metabolites of interest γ-ATP and P_i.

This study has certain limitations:

1. For the day-to-day reproducibility study there was no randomization of the protocols and coils, which might lead to a bias if customization to the measurements is needed. However, all the volunteers were familiar with MRS studies. Furthermore, all volunteers left the scanner after the single loop coil measurement without markers, allowing for identification of the coil setup. Thus, positioning of the quadrature coil was performed independently from the previous setup.
2. This study did not apply a correction for liver lipid content, which is usually performed for hepatic ATP measurements. However, the participants had a stable lifestyle without changes in meal pattern and physical activity during the short period of this study. Thus, hepatic lipid content will not affect the reproducibility and consistency of results under these conditions. Still, it might have influenced the spread of the obtained data, especially in the case of the two obese volunteers.

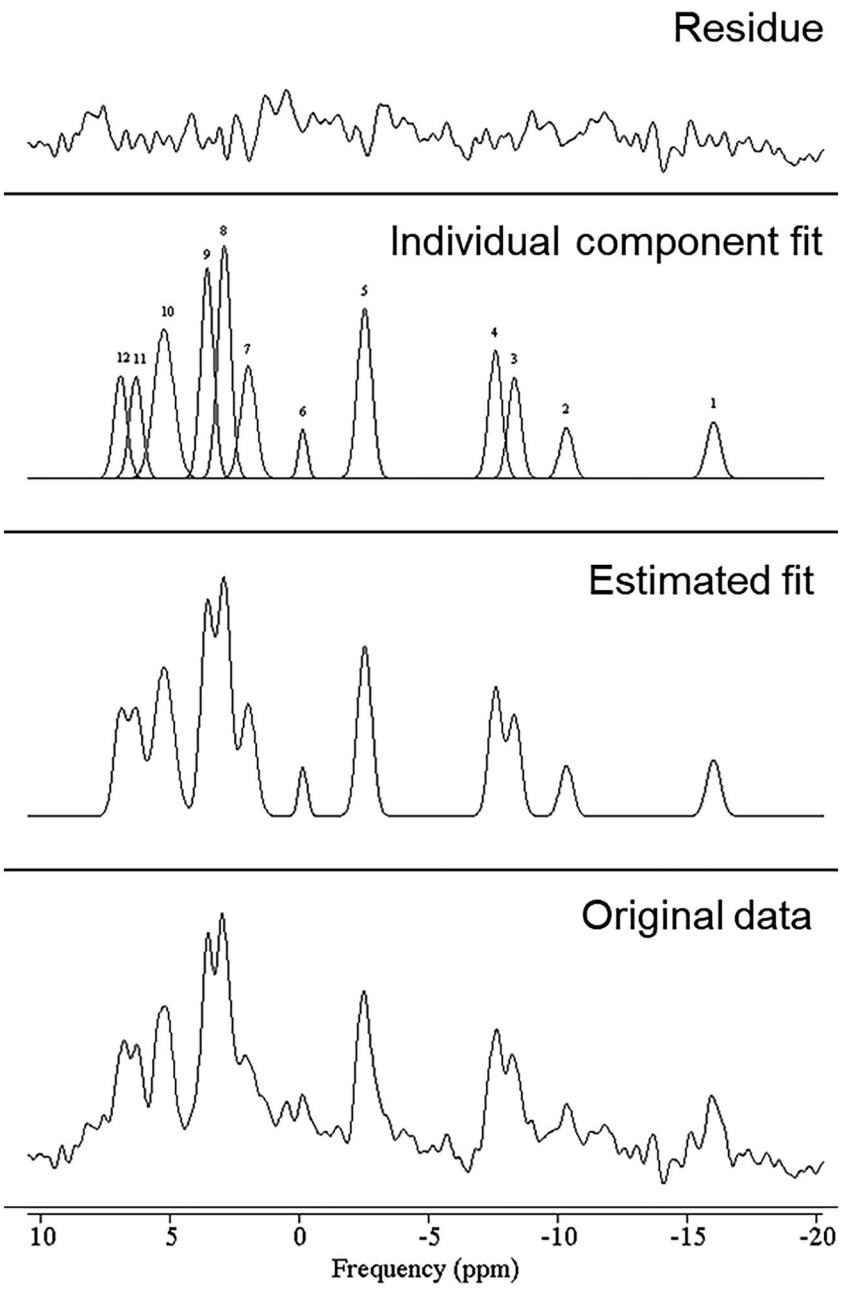

FIGURE 6 Exemplary result of the advanced method for accurate, robust, and efficient spectral fitting (AMARES) fitting routine of a human hepatic ^{31}P-spectrum (quadrature coil). Graphs from bottom to top: original data, sum of fitting result, individual peak fitting (1,4,5: β-,α-,γ-adenosine triphosphate [ATP], 2: uridine diphosphate glucose [UDPG], 3: nicotinamide adenine dinucleotide (phosphate) [NAD(P)H], 6: phosphocreatine [PCr], 7: phosphoenolpyruvate/phosphatidylcholine [PEP/PtdC], 8,9: phosphodiester [PDE], 10: inorganic phosphate [P_i], 11,12: phosphomonoester [PME]) and residue of the spectrum after fitting.

3. The obtained absolute concentrations for both γ-ATP and P_i are slightly lower compared with previous data of our group.[36] Lower absolute concentrations may result from the absence of correction for liver lipid content or from a different duration of fasting before the measurements. Nevertheless, dietary intervention studies revealed conflicting results on meal ingestion and fasting on ATP concentrations.[16,23,53,54]
4. A recent publication indicated that the absolute concentrations obtained using the phantom replacement technique can be biased when the conductivity of the phantom does not match the in vivo situation.[49] An acceptable range of conductivity of a phosphate phantom at 3-T field strength was found to be between $0.39-0.58\,\frac{S}{m}$. The 50 mM K_2HPO_4 phantom used in this study has an estimated conductivity of appoximately $0.89\,\frac{S}{m}$, which may introduce a 20% bias. Correcting our results according to Purvis et al.[49] would lead to concentrations of 2.78 and 2.08 mM for γ-ATP and P_i, which is still in agreement with the literature.

In summary, 3D-ISIS ^{31}P-MRS allows for robust measurement of hepatic γ-ATP and P_i concentrations within a reasonable time frame of ∼13 min when a single loop or a quadrature coil is used. High reproducibility was shown for both day-to-day (CV < 11%) and intra-day studies with full repositioning (CV < 8%). The similarity of the metabolite concentrations between both coils and visits shows the robustness of the phantom-replacement method for obtaining absolute concentrations. This justifies switching between coils without introducing a coil-dependent bias. The larger coil loops of the quadrature coil may increase the success rate of measurements in people with obesity and in those with BMI values exceeding 32 kg/m^2.

AUTHOR CONTRIBUTIONS

Marc Jonuscheit designed the study, conducted the measurements, analyzed and interpreted the data, and wrote the manuscript. Stefan Wierichs analyzed the data and reviewed/edited the manuscript. Maik Rothe conducted the measurements and reviewed/edited the manuscript. Julian Mevenkamp helped with data analysis. Pavel Bobrov performed statistical analysis. Benedict Korzekwa, Yuliya Kupriyanova, and Michael Roden reviewed/edited the manuscript. Vera B. Schrauwen-Hinderling supervised the study, interpreted data, and reviewed/edited the manuscript. Vera B. Schrauwen-Hinderling is the guarantor of this work and, as such, had full access to all the data in the study and takes responsibility for the integrity of the data and the accuracy of the data analysis. All authors read and approved the final manuscript.

ACKNOWLEDGMENTS

The authors thank Prof. Oliver Kuß, Institute for Biometrics and Epidemiology, German Diabetes Center at Heinrich Heine University, for helpful discussions.

CONFLICT OF INTEREST STATEMENT

MR received lecture fees and/or served on advisory boards for Astra-Zeneca, Boehringer-Ingelheim, Eli Lilly, Novartis, Novo Nordisk, and Target RWE. No conflicts of interest, financial or otherwise, are declared by the other authors.

ORCID

Marc Jonuscheit https://orcid.org/0009-0003-3875-3382

REFERENCES

1. Cox IJ, Menon DK, Sargentoni J, et al. Phosphorus-31 magnetic resonance spectroscopy of the human liver using chemical shift imaging techniques. *J Hepatol.* 1992;14(2–3):265-275. doi:10.1016/0168-8278(92)90169-P
2. Menon DK, Sargentoni J, Taylor-Robinson SD, et al. Effect of functional grade and etiology onin vivo hepatic phosphorus-31 magnetic resonance spectroscopy in cirrhosis: biochemical basis of spectral appearances. *Hepatology*. 1995;21(2):417-427. doi:10.1002/hep.1840210224
3. Munakata T, Griffiths RD, Martin PA, Jenkins SA, Shields R, Edwards RH. An in vivo ^{31}P MRS study of patients with liver cirrhosis: progress towards a non-invasive assessment of disease severity. *NMR Biomed.* 1993;6(2):168-172. doi:10.1002/nbm.1940060211
4. Meyerhoff DJ, Boska MD, Thomas AM, Weiner MW. Alcoholic liver disease: quantitative image-guided P-31 MR spectroscopy. *Radiology*. 1989; 173(2):393-400. doi:10.1148/radiology.173.2.2798871
5. Corbin IR, Ryner LN, Singh H, Minuk GY. Quantitative hepatic phosphorus-31 magnetic resonance spectroscopy in compensated and decompensated cirrhosis. *Am J Physiol Gastrointest Liver Physiol.* 2004;287(2):G379-G384. doi:10.1152/ajpgi.00418.2003
6. Rajanayagam V, Lee RR, Ackerman Z, Bradley WG, Ross BD. Quantitative P-31 MR spectroscopy of the liver in alcoholic cirrhosis. *J Magn Reson Imaging.* 1992;2(2):183-190. doi:10.1002/jmri.1880020211
7. Dixon RM, Angus PW, Rajagopalan B, Radda GK. Abnormal phosphomonoester signals in ^{31}P MR spectra from patients with hepatic lymphoma. A possible marker of liver infiltration and response to chemotherapy. *Br J Cancer.* 1991;63(6):953-958. doi:10.1038/bjc.1991.208
8. Wolf P, Fellinger P, Pfleger L, et al. Reduced hepatocellular lipid accumulation and energy metabolism in patients with long standing type 1 diabetes mellitus. *Sci Rep.* 2019;9(1):2576. doi:10.1038/s41598-019-39362-4
9. Gancheva S, Bierwagen A, Kaul K, et al. Variants in genes controlling oxidative metabolism contribute to lower hepatic ATP independent of liver fat content in type 1 diabetes. *Diabetes.* 2016;65(7):1849-1857. doi:10.2337/db16-0162
10. Kupriyanova Y, Zaharia OP, Bobrov P, et al. Early changes in hepatic energy metabolism and lipid content in recent-onset type 1 and 2 diabetes mellitus. *J Hepatol.* 2021;74(5):1028-1037. doi:10.1016/j.jhep.2020.11.030

11. Solga SF, Horska A, Hemker S, et al. Hepatic fat and adenosine triphosphate measurement in overweight and obese adults using ^{1}H and ^{31}P magnetic resonance spectroscopy. *Liver Int*. 2008;28(5):675-681. doi:10.1111/j.1478-3231.2008.01705.x
12. Schmid AI, Szendroedi J, Chmelik M, Krssák M, Moser E, Roden M. Liver ATP synthesis is lower and relates to insulin sensitivity in patients with type 2 diabetes. *Diabetes Care*. 2011;34(2):448-453. doi:10.2337/dc10-1076
13. Szendroedi J, Chmelik M, Schmid AI, et al. Abnormal hepatic energy homeostasis in type 2 diabetes. *Hepatology*. 2009;50(4):1079-1086. doi:10.1002/hep.23093
14. Sarabhai T, Mastrototaro L, Kahl S, et al. Hyperbaric oxygen rapidly improves tissue-specific insulin sensitivity and mitochondrial capacity in humans with type 2 diabetes: a randomised placebo-controlled crossover trial. *Diabetologia*. 2023;66(1):57-69. doi:10.1007/s00125-022-05797-0
15. Gancheva S, Koliaki C, Bierwagen A, et al. Effects of intranasal insulin on hepatic fat accumulation and energy metabolism in humans. *Diabetes*. 2015;64(6):1966-1975. doi:10.2337/db14-0892
16. Fritsch M, Koliaki C, Livingstone R, et al. Time course of postprandial hepatic phosphorus metabolites in lean, obese, and type 2 diabetes patients. *Am J Clin Nutr*. 2015;102(5):1051-1058. doi:10.3945/ajcn.115.107599
17. Norén B, Lundberg P, Ressner M, Wirell S, Almer S, Smedby O. Absolute quantification of human liver metabolite concentrations by localized in vivo ^{31}P NMR spectroscopy in diffuse liver disease. *Eur Radiol*. 2005;15(1):148-157. doi:10.1007/s00330-004-2434-x
18. Fellinger P, Wolf P, Pfleger L, et al. Increased ATP synthesis might counteract hepatic lipid accumulation in acromegaly. *JCI Insight*. 2020;5(5):e134638. doi:10.1172/jci.insight.134638
19. Gancheva S, Caspari D, Bierwagen A, et al. Cardiometabolic risk factor clustering in patients with deficient branched-chain amino acid catabolism: a case-control study. *J Inherit Metab Dis*. 2020;43(5):981-993. doi:10.1002/jimd.12231
20. Wylezinska M, Cobbold JFL, Fitzpatrick J, et al. A comparison of single-voxel clinical in vivo hepatic ^{31}P MR spectra acquired at 1.5 and 3.0 Tesla in health and diseased states. *NMR Biomed*. 2011;24(3):231-237. doi:10.1002/nbm.1578
21. Zakian KL, Koutcher JA, Malhotra S, et al. Liver regeneration in humans is characterized by significant changes in cellular phosphorus metabolism: assessment using proton-decoupled ^{31}P-magnetic resonance spectroscopic imaging. *Magn Reson Med*. 2005;54(2):264-271. doi:10.1002/mrm.20560
22. Oberhaensli RD, Galloway GJ, Hilton-Jones D, et al. The study of human organs by phosphorus-31 topical magnetic resonance spectroscopy. *Br J Radiol*. 1987;60(712):367-373. doi:10.1259/0007-1285-60-712-367
23. Hakkarainen A, Lundbom J, Tuominen EK, Taskinen M-R, Pietiläinen KH, Lundbom N. Measuring short-term liver metabolism non-invasively: post-prandial and post-exercise ^{1}H and ^{31}P MR spectroscopy. *MAGMA*. 2015;28(1):57-66. doi:10.1007/s10334-014-0450-7
24. Hultman E, von Nilsson LH, Sahlin K. Adenine nucleotide content of human liver. Normal values and fructose-induced depletion. *Scand J Clin Lab Invest*. 1975;35(3):245-251. doi:10.3109/00365517509095736
25. Sijens PE, Dagnelie PC, Halfwerk S, van Dijk P, Wicklow K, Oudkerk M. Understanding the discrepancies between ^{31}P MR spectroscopy assessed liver metabolite concentrations from different institutions. *Magn Reson Imaging*. 1998;16(2):205-211. doi:10.1016/S0730-725X(97)00246-4
26. Purvis LAB, Clarke WT, Valkovič L, et al. Phosphodiester content measured in human liver by in vivo ^{31}P MR spectroscopy at 7 Tesla. *Magn Reson Med*. 2017;78(6):2095-2105. doi:10.1002/mrm.26635
27. Schmid AI, Chmelík M, Szendroedi J, et al. Quantitative ATP synthesis in human liver measured by localized ^{31}P spectroscopy using the magnetization transfer experiment. *NMR Biomed*. 2008;21(5):437-443. doi:10.1002/nbm.1207
28. Buehler T, Kreis R, Boesch C. Comparison of ^{31}P saturation and inversion magnetization transfer in human liver and skeletal muscle using a clinical MR system and surface coils. *NMR Biomed*. 2015;28(2):188-199. doi:10.1002/nbm.3242
29. Meyerhoff DJ, Karczmar GS, Matson GB, Boska MD, Weiner MW. Non-invasive quantitation of human liver metabolites using image-guided ^{31}P magnetic resonance spectroscopy. *NMR Biomed*. 1990;3(1):17-22. doi:10.1002/nbm.1940030103
30. Buchli R, Meier D, Martin E, Boesiger P. Assessment of absolute metabolite concentrations in human tissue by ^{31}P MRS in vivo. Part II: muscle, liver, kidney. *Magn Reson Med*. 1994;32(4):453-458. doi:10.1002/mrm.1910320405
31. Chmelík M, Schmid AI, Gruber S, et al. Three-dimensional high-resolution magnetic resonance spectroscopic imaging for absolute quantification of ^{31}P metabolites in human liver. *Magn Reson Med*. 2008;60(4):796-802. doi:10.1002/mrm.21762
32. Pfleger L, Gajdošík M, Wolf P, et al. Absolute quantification of phosphor-containing metabolites in the liver using ^{31}P MRSI and hepatic lipid volume correction at 7T suggests no dependence on body mass index or age. *J Magn Reson Imaging*. 2019;49(2):597-607. doi:10.1002/jmri.26225
33. Hoult DI, Chen CN, Sank VJ. Quadrature detection in the laboratory frame. *Magn Reson Med*. 1984;1(3):339-353. doi:10.1002/mrm.1910010305
34. Szendroedi J, Saxena A, Weber KS, et al. Cohort profile: the German Diabetes Study (GDS). *Cardiovasc Diabetol*. 2016;15:59. doi:10.1186/s12933-016-0374-9
35. Zaharia OP, Strassburger K, Knebel B, et al. Role of patatin-like phospholipase domain-containing 3 gene for hepatic lipid content and insulin resistance in diabetes. *Diabetes Care*. 2020;43(9):2161-2168. doi:10.2337/dc20-0329
36. Laufs A, Livingstone R, Nowotny B, et al. Quantitative liver ^{31}P magnetic resonance spectroscopy at 3T on a clinical scanner. *Magn Reson Med*. 2014;71(5):1670-1675. doi:10.1002/mrm.24835
37. Ordidge R, Connelly A, Lohman J. Image-selected in vivo spectroscopy (ISIS). A new technique for spatially selective NMR spectroscopy. *J Magn Reson*. 1986;66(2):283-294. doi:10.1016/0022-2364(86)90031-4
38. Lin A, Andronesi O, Bogner W, et al. Experts' Working Group on Reporting Standards for MR Spectroscopy Minimum reporting standards for in vivo magnetic resonance spectroscopy (MRSinMRS): experts' consensus recommendations. *NMR Biomed*. 2021;34(5):e4484. doi:10.1002/nbm.4484
39. Kreis R, Boer V, Choi I-Y, et al. Experts' Working Group on Terminology for MR Spectroscopy Terminology and concepts for the characterization of in vivo MR spectroscopy methods and MR spectra: background and experts' consensus recommendations. *NMR Biomed*. 2020;34(5):e4347. doi:10.1002/nbm.4347
40. Naressi A, Couturier C, Castang I, de Beer R, Graveron-Demilly D. Java-based graphical user interface for MRUI, a software package for quantitation of in vivo/medical magnetic resonance spectroscopy signals. *Comput Biol Med*. 2001;31(4):269-286. doi:10.1016/S0010-4825(01)00006-3
41. Stefan D, Cesare FD, Andrasescu A, et al. Quantitation of magnetic resonance spectroscopy signals: the jMRUI software package. *Meas Sci Technol*. 2009;20(10):104035. doi:10.1088/0957-0233/20/10/104035
42. Mierisová S, van den Boogaart A, Tkác I, van Hecke P, Vanhamme L, Liptaj T. New approach for quantitation of short echo time in vivo ^{1}H MR spectra of brain using AMARES. *NMR Biomed*. 1998;11(1):32-39. doi:10.1002/(SICI)1099-1492(199802)11:13.0.CO;2-#

43. Vanhamme L, van den Boogaart A, van Huffel S. Improved method for accurate and efficient quantification of MRS data with use of prior knowledge. *J Magn Reson*. 1997;129(1):35-43. doi:10.1006/jmre.1997.1244
44. Li CW, Negendank WG, Murphy-Boesch J, Padavic-Shaller K, Brown TR. Molar quantitation of hepatic metabolites in vivo in proton-decoupled, nuclear Overhauser effect enhanced ^{31}P NMR spectra localized by three-dimensional chemical shift imaging. *NMR Biomed*. 1996;9(4):141-155. doi:10.1002/(SICI)1099-1492(199606)9:43.0.CO;2-P
45. de Graaf RA. *In Vivo NMR Spectroscopy: Principles and Techniques*. 2nd ed. John Wiley & Sons; 2013. http://gbv.eblib.com/patron/FullRecord.aspx?p=4037486
46. Stroup WW. *Generalized Linear Mixed Models: Modern Concepts, Methods and Applications*. Chapman and Hall/CRC Texts in Statistical Science Ser. CRC Press; 2013. https://ebookcentral.proquest.com/lib/kxp/detail.action?docID=1570060
47. Tosner Z, Dezortová M, Tintěra J, Hájek M. Application of two-dimensional CSI for absolute quantification of phosphorus metabolites in the human liver. *MAGMA*. 2001;13(1):40-46. doi:10.1007/BF02668649
48. Bashir A, Gropler R, Ackerman J. Absolute quantification of human liver phosphorus-containing metabolites in vivo using an inhomogeneous spoiling magnetic field gradient. *PLoS ONE*. 2015;10(12):e0143239. doi:10.1371/journal.pone.0143239
49. Purvis LAB, Valkovič L, Robson MD, Rodgers CT. Feasibility of absolute quantification for ^{31}P MRS at 7 T. *Magn Reson Med*. 2019;82(1):49-61. doi:10.1002/mrm.27729
50. Bierwagen A, Begovatz P, Nowotny P, et al. Characterization of the peak at 2.06 ppm in ^{31}P magnetic resonance spectroscopy of human liver: phosphoenolpyruvate or phosphatidylcholine? *NMR Biomed*. 2015;28(7):898-905. doi:10.1002/nbm.3323
51. Chmelík M, Valkovič L, Wolf P, et al. Phosphatidylcholine contributes to in vivo ^{31}P MRS signal from the human liver. *Eur Radiol*. 2015;25(7):2059-2066. doi:10.1007/s00330-014-3578-y
52. Sedivy P, Dusilova T, Hajek M, Burian M, Krššák M, Dezortova M. In vitro ^{31}P MR chemical shifts of in vivo-detectable metabolites at 3T as a basis set for a pilot evaluation of skeletal muscle and liver ^{31}P spectra with LCModel software. *Molecules*. 2021;26(24):7571. doi:10.3390/molecules26247571
53. Hernández EÁ, Kahl S, Seelig A, et al. Acute dietary fat intake initiates alterations in energy metabolism and insulin resistance. *J Clin Invest*. 2017;127(2):695-708. doi:10.1172/JCI89444
54. Bawden SJ, Stephenson MC, Ciampi E, et al. Investigating the effects of an oral fructose challenge on hepatic ATP reserves in healthy volunteers: a (31)P MRS study. *Clin Nutr*. 2016;35(3):645-649. doi:10.1016/j.clnu.2015.04.001

SUPPORTING INFORMATION

Additional supporting information can be found online in the Supporting Information section at the end of this article.

How to cite this article: Jonuscheit M, Wierichs S, Rothe M, et al. Reproducibility of absolute quantification of adenosine triphosphate and inorganic phosphate in the liver with localized ^{31}P-magnetic resonance spectroscopy at 3-T using different coils. *NMR in Biomedicine*. 2024;37(8):e5120. doi:10.1002/nbm.5120